RSC Advances

PAPER

View Article Online
View Journal | View Issue

Cite this: *RSC Adv.*, 2020, **10**, 11535

Shape engineering of polystyrene particles from spherical to raspberry-like to hollow flower-like *via* one-step non-surfactant self-templating polymerization of styrene in ethanol–water mixtures†

Xuechen Xiang, Zhe Chen, Dongfang Ren, Jiaqiong Xu, Xiaofeng Li, Zixin Ye, Ning Chen, Qiming Chen* and Shiyu Ma*

Received 1st January 2020
Accepted 27th February 2020

DOI: 10.1039/d0ra00005a

rsc.li/rsc-advances

We report a facile method for preparation of polystyrene (PS) particles with spherical, raspberry-like, and hollow flower-like structures by single-step non-surfactant self-templating polymerization of styrene in ethanol–water mixtures. PS particles with diverse morphologies could be easily obtained by simply adjusting the volume ratios of the styrene/water/ethanol mixture and initiator-ethanol–water mixture. By decreasing this ratio, the particles with spherical, raspberry-like, and hollow flower-like structures were obtained in sequence. The wettability of the coatings changing from hydrophilicity to hydrophobicity was easily tuned by the PS particles with different roughnesses. A competitive mechanism of interfacial polymerization and exudation was proposed to interpret the formation of PS particles with diverse morphologies.

1 Introduction

Synthesis of asymmetric non-spherical nanomaterials with controllable morphologies has become a hot topic of research.[1] Non-spherical morphologies endow materials with enhanced physical and chemical properties, such as mechanical strength, thermal stability, good adsorptivity, catalytic activity,[2] and rheological properties.[3] To date, PS particles with different non-spherical shapes, such as bowl-like,[4] raspberry-like,[5] flower-like,[2] peanut-like,[6] snowman-like, and triple rod particles[7] have been synthesized. Due to their unique hierarchical structures, designed surface properties, and high surface roughness, raspberry-like and flower-like particles have always been used to enhance Raman scattering, separation, and heterogeneous catalysis and also to enhance the efficiency of the drug delivery system. As the most promising building blocks, they have also been used for the fabrication of superhydrophobic coatings.[5]

Recently, various approaches including surfactant-free emulsion polymerization,[5,12] miniemulsion polymerization,[11] seeded emulsion polymerization,[13,14] electrostatic adsorption,[9,10] layer-by-layer templating,[16,41] and self-assembly methods[8] have been developed to construct raspberry-like and flower-like hierarchical structures. Fan *et al.* prepared a series of raspberry-like poly(styrene-acrylic acid) particles by changing the molar ratios of styrene and acrylic acid in a soap-free emulsion polymerization process.[5] Huang *et al.* prepared a series of raspberry-like polystyrene/carbon black composite microspheres by changing the π–π interactions during the mixing process.[15] Dong *et al.* transformed the microspheres from raspberry-like to flower-like morphology by simply adjusting the stoichiometry of the silane precursor.[17] Uniformly-sized hierarchical spheres could be obtained by these methods. And nowadays, a kind of ternary system such as monomer/water/methanol system has been used in polymer latex preparation.[31,32] However, the mechanism of polymerization in ternary system is not clear and it is still a challenge to prepare PS particles with controlled morphologies in ternary system due to the existence of liquid/liquid and liquid/solid interfacial tension.

Herein, we demonstrate a facile, one-step route to synthesize single-component PS particles with diverse morphologies by altering the volume ratios of styrene/water/ethanol mixture to initiator-ethanol–water mixture. Using this non-surfactant self-templating polymerization process, PS particles with spherical, raspberry-like, and hollow flower-like structures were prepared. A further study was made on the range of proportions for each shape. The formation of PS particles with diverse morphologies might be determined by a competitive process of interfacial

Research Center of Water Resources and Interface Science, School of Chemistry and Molecular Engineering, East China Normal University, No. 500, Dongchuan Rd., Shanghai 200241, P. R. China. E-mail: qmchen@chem.ecnu.edu.cn; syma@chem.ecnu.edu.cn

† Electronic supplementary information (ESI) available: TEM images of PS particles prepared with $R = 1/15.03/17.86$ ($V_M : V_I = 1 : 0.15$) at 250 rpm; DLS results of the as-prepared PS particles. TEM images of the PS particles prepared with $V_M : V_I = 1 : 9$ in different system; TEM images of PS particles prepared with $V_M : V_I = 1 : 15$ in different system; DLS results for oil droplets in the system of $V_M : V_E = 1 : 13$ at different aging time; DLS results for oil droplets in the system of $V_M : V_E = 1 : 15$ at different aging time; FT-IR spectra of the as-prepared PS particles. See DOI: 10.1039/d0ra00005a

polymerization and exudation in oil droplets. The surface coated with these particles of hierarchical structures showed tunable wettability that could be changed from hydrophilicity (water contact angle, 62.5°) to hydrophobicity (water contact angle, 134.5°).

2 Experimental section

2.1 Materials

Styrene (St, 99.5%, AR, Sinopharm Chemical Reagent Co. Ltd) was purified by distillation under reduced pressure and stored in a refrigerator prior to use. Absolute ethanol (EtOH, 99.7%, AR), methanol (99.7%, GR), isopropanol (99.7%, AR), and *tert*-butanol (98%, CP) were procured from Sinopharm Chemical Reagent Co. Ltd Potassium persulfate (KPS, 99.5%, AR, Sinopharm Chemical Reagent Co. Ltd) and sodium bisulfite ($NaHSO_3$, 99.99%, Shanghai Aladdin Biochemical Technology Co. Ltd) were used as a dual initiator system in this study. Ultrapure water (H_2O) with resistivity higher than 18.2 MΩ cm was used throughout the study. Argon gas was bubbled into the water to remove dissolved oxygen.

2.2 Preparation of PS particles with diverse morphologies

PS particles with diverse morphologies were prepared by a one-step non-surfactant self-templating polymerization process. The details of experimental procedures used in this paper are presented in Table 1. In a typical procedure, styrene (3.5 mL), water (40 mL), and ethanol (60 mL) (ratio of mass fraction (R) of St/H_2O/EtOH = 2.95/44.34/52.71) were added into a flask, and stirred at 50 rpm in argon atmosphere till the mixture turned transparent. This formed the initial St/H_2O/EtOH ternary system (called Monomer Mixture, MM, the volume of MM was represented as V_M). The initiator solution (the volume of initiator solution was represented as V_I) was a mixture of EtOH and H_2O ($V_{EtOH} : V_{H_2O} = 3 : 2$) containing radicals, which were obtained from redox initiator. Small aliquots of MM (*ca.* 10 mL) were taken in Erlenmeyer flasks and covered with a plug, and mixed with different volumes of initiator solution and reacted at 25 °C for 7 days. The PS particles with diverse morphologies were obtained. After washing with H_2O and EtOH, PS particles were used to fabricate the hierarchical structured coatings.

2.3 Assembly of hierarchical structured coatings

Prior to experiment, glass slides with dimensions of 20 × 20 mm^2 were treated with piranha solution (a mixture containing 98% concentrated sulfuric acid and 30% hydrogen peroxide in 7 : 3 v/v) at 80 °C for 2 h and rinsed thoroughly with water to remove any contaminants (**Warning**: the piranha solution has strong oxidizing properties and it reacts violently with organic materials). The obtained PS suspensions were centrifuged, washed with H_2O and EtOH and diluted with water to obtain 0.2 wt% concentration, and sonicated to obtain uniform dispersions. A glass slide was vertically immersed into each of the PS suspensions in a vial.[5] Then, the vials were vertically placed in a constant temperature chamber at 25 °C for 7 days to completely evaporate the water present in the suspensions. The coatings were obtained after water evaporation, leaving deposition of particles on the glass slides.

2.4 Characterization

Scanning electron microscopic (SEM) and transmission electron microscopic (TEM) images were recorded using Hitachi S-4800 microscope and JEOLJEM-2100 microscope, respectively. The particle size distribution of the PS particles dispersed in water was determined by dynamic light scattering technique (DLS, Zetasizer Nano ZS, Malvern Panalytical Company). Atomic force microscopy (AFM) was conducted on Bruker Multimode 8. FT-IR spectra of the as-prepared PS particles were recorded by Nicolet Fourier transform infrared spectrometer (NEXUS 670) using the KBr technique. The images of water contact angles were obtained using JC2000D1 contact angle analyzer (Powereach, China) with ultrapure water droplet size of 8 μL at room temperature. All the contact angle values were determined as averages of measurements from at least five different points on each sample surface, using the Laplace–Young fitting mode.

3 Results and discussion

3.1 Synthesis of PS particles with diverse morphologies

PS particles with smooth surfaces have been extensively fabricated for various purposes over the past few decades. However, rough surface particles with great potential applications require further research. Herein, a simple method of synthesis of PS

Table 1 Detailed experimental conditions of the preparation of PS particles with diverse morphologies

	Monomer mixture			Initiator solution					
Sample	Styrene/mL	Ethanol–water mixture/mL	V_M/mL	C(KPS)/g mL^{-1}	$C(NaHSO_3)$/g mL^{-1}	Ethanol–water mixture/mL	V_I/mL	$V_M : V_I$	Styrene/water/ethanol mass fraction ratio (R)
1	0.34	9.66	10	6.32×10^{-4}	4.10×10^{-4}	1.5	1.5	1 : 0.15	2.95/44.34/52.71
2	0.34	9.66	10	6.32×10^{-4}	4.10×10^{-4}	20	20	1 : 2	1.13/45.22/53.65
3	0.34	9.66	10	6.32×10^{-4}	4.10×10^{-4}	30	30	1 : 3	0.85/45.53/53.62
4	0.34	9.66	10	6.32×10^{-4}	4.10×10^{-4}	90	90	1 : 9	0.34/45.58/54.08
5	0.34	9.66	10	6.32×10^{-4}	4.10×10^{-4}	120	120	1 : 12	0.26/45.62/54.12
6	0.34	9.66	10	6.32×10^{-4}	4.10×10^{-4}	130	130	1 : 13	0.24/45.63/54.13
7	0.34	9.66	10	6.32×10^{-4}	4.10×10^{-4}	150	150	1 : 15	0.21/45.64/54.12
8	0.34	9.66	10	6.32×10^{-4}	4.10×10^{-4}	190	190	1 : 19	0.17/45.66/54.17

particles with diverse morphologies is reported, which have been designed by adjusting the ratio of V_M to V_I.

The process for the preparation of PS particles with diverse morphologies is shown in Scheme 1. Styrene, water, and ethanol were taken in a reaction flask and blended to obtain a uniform and transparent mixture. By keeping V_M constant and changing V_I, PS particles with spherical, raspberry-like, and hollow flower-like structures could be obtained.

Fig. 1 presents TEM and SEM images of the obtained PS particles. By changing the ratio of V_M to V_I, three typical morphologies of PS particles could be prepared. Sample 1 ($V_M : V_I = 1 : 0.15$, Fig. 1a and d) with smooth spherical structures were obtained. The diameters of the PS particles were about 250 nm (Fig. 2), which were much larger than expected. This might be due to the aggregation of the colliding particles in the absence of shear force.[33] When the stirring speed used was set up at 250 rpm, the PS particles with 220 nm in diameter and good monodispersity were obtained (Fig. S1†). The surface of Sample 4 ($V_M : V_I = 1 : 9$, Fig. 1b and e) were rough and heterogeneous. The size of raspberry-like particles was reduced to 180 nm (Fig. 2). Sample 8 ($V_M : V_I = 1 : 19$, Fig. 1c and f) with hollow flower-like structures were obtained. The particle size was only 132 nm (Fig. 2). The possible formation process of the hollow PS particles was as follows: the polystyrene on the surface of PS particle was more physically robust than that of the interiors. In other words, the interior of particles was "softer" and possessed a loose structure, due to lower degree of polymerization in the polymerization process. Whereas, the shell was "harder" with a dense structure, due to a higher degree of polymerization.[18–23] St monomers and short oligomers in the interior of particles could be extracted when the EtOH–H_2O mixture was added to the MM.

Fig. 3 shows TEM images of the PS particles prepared by different $V_M : V_I$ ratios in detail. Sample 1 ($V_M : V_I = 1 : 0.15$, Fig. 3a) had a smooth surface. Sample 2 ($V_M : V_I = 1 : 2$, Fig. 3b) showed poor surface smoothness compared to that of Sample 1. There are some depressions and bulges on the surface of

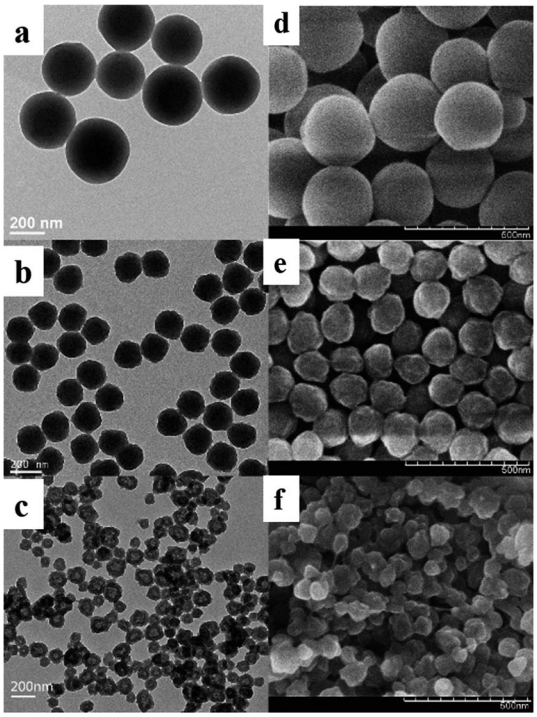

Fig. 1 TEM (a–c) and SEM (d–f) images of Sample 1 (a and d, $V_M : V_I = 1 : 0.15$), Sample 4 (b and e, $V_M : V_I = 1 : 9$), and Sample 8 (c and f, $V_M : V_I = 1 : 19$).

Sample 3 ($V_M : V_I = 1 : 3$, Fig. 3c). Therefore, spherical particles could be prepared by maintaining the $V_M : V_I$ less than or equal to 1 : 2. From Sample 3 ($V_M : V_I = 1 : 3$, Fig. 3c) to Sample 5 ($V_M : V_I = 1 : 12$, Fig. 3e), the lower the ratio of $V_M : V_I$, the higher the roughness of surface. For Sample 6 ($V_M : V_I = 1 : 13$, Fig. 3f), a very small hollow domain appeared in several particles. For Sample 7 ($V_M : V_I = 1 : 15$, Fig. 3g), the hollow domains present in all particles. Thence, raspberry-like particles could be obtained when $V_M : V_I$ was between 1 : 12 and 1 : 3, whereas hollow flower-like particles could be prepared by maintaining

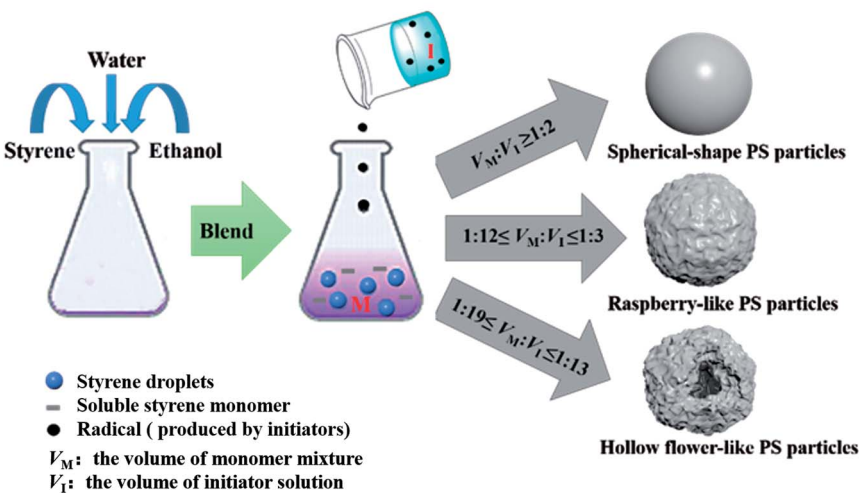

Scheme 1 Schematic illustration of the synthesis process for PS particles with different morphologies.

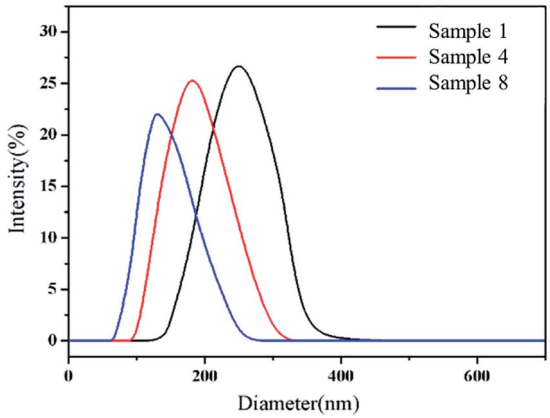

Fig. 2 DLS results of Sample 1 ($V_M : V_I = 1 : 0.15$), Sample 4 ($V_M : V_I = 1 : 9$) and Sample 8 ($V_M : V_I = 1 : 19$).

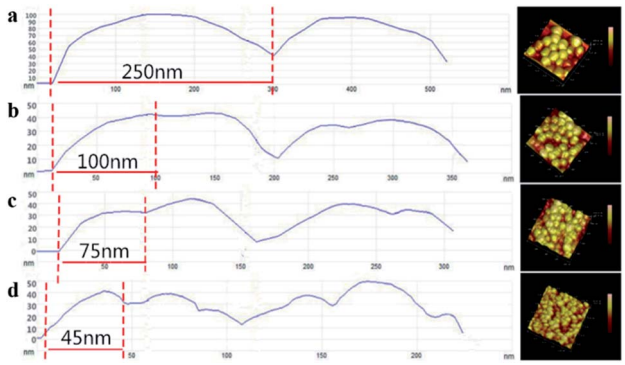

Fig. 4 AFM images and the surface structures of different samples: (a) Sample 1 ($V_M : V_I = 1 : 0.15$); (b) Sample 4 ($V_M : V_I = 1 : 9$); (c) Sample 6 ($V_M : V_I = 1 : 13$); (d) Sample 8 ($V_M : V_I = 1 : 19$).

$V_M : V_I$ between 1 : 19 and 1 : 13. Moreover, particle size decreased as the ratio of V_M to V_I decreased (Fig. S2†). When the ratio of V_M to V_I decreased, the mass fraction of St monomer in the mixture decreased, along with a corresponding decrease in the size of oil droplets. Especially, the hollow area of the PS particles increased as the ratio decreased.

At the same time, it was noticed that as the ratio decreased, the roughness of the particle surface increased. In order to describe the differences in roughness, the products were characterized by AFM. Fig. 4 shows the AFM images processed by NanoScope Analysis 1.5 software, in which the section function was used to display the surface conditions of the two adjacent particles. Each curve was statistically derived from 50 sets of data points. The length of the smallest bump on the curve was included in the description of diverse roughness. For Sample 1 ($V_M : V_I = 1 : 0.15$, Fig. 4a), the curve was smooth and the bump was around 250 nm in length, which was similar to the size of the spherical PS particles obtained. For Sample 4 ($V_M : V_I = 1 : 9$, Fig. 4b), a bump, approximately 100 nm in size, which was smaller than the particle size. For Sample 8 ($V_M : V_I = 1 : 19$, Fig. 4d), the curves were coarser and had more obvious bumps of about 45 nm size. For Sample 6 ($V_M : V_I = 1 : 13$, Fig. 4c), the particles had raspberry-like structures, but the bumps were about 75 nm in size, which were larger than that of Sample 8 ($V_M : V_I = 1 : 19$). Thus, when the ratio of V_M to V_I decreased, roughness of the particle surface increased.

The effects of other soluble alcohols (methanol, isopropanol, and *tert*-butanol) on morphologies of PS particles were also investigated. Fig. S3 and S4† show TEM images of the PS particles prepared in styrene/water/methanol ternary system, styrene/water/isopropanol ternary system, and styrene/water/*tert*-butanol ternary system. The results showed that the roughness of PS particles increased as the ratio of V_M to V_I decreased, and different alcohols had different effects on the morphologies of PS particles.

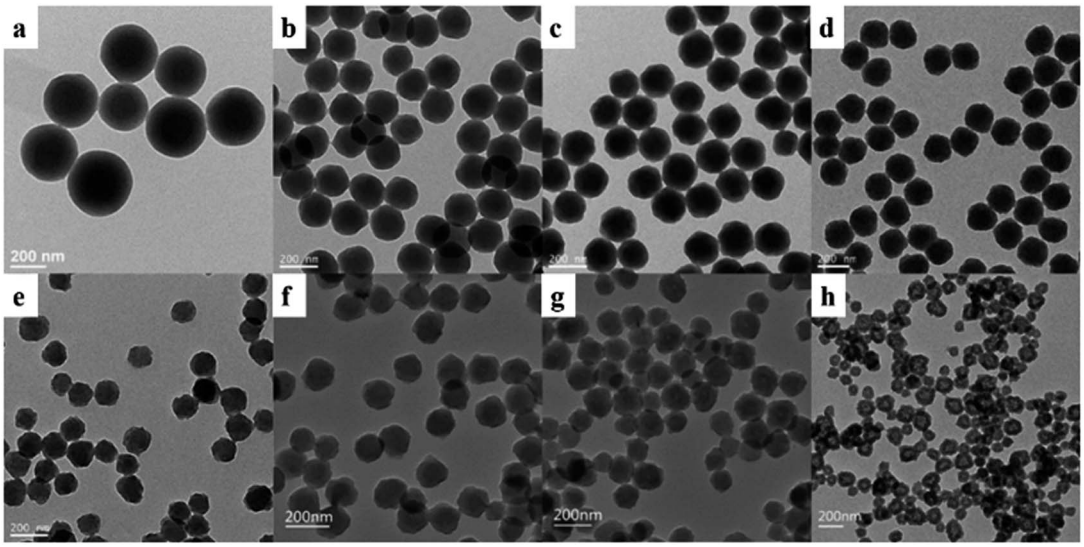

Fig. 3 TEM images of different samples: (a) Sample 1 ($V_M : V_I = 1 : 0.15$); (b) Sample 2 ($V_M : V_I = 1 : 2$); (c) Sample 3($V_M : V_I = 1 : 3$); (d) Sample 4 ($V_M : V_I = 1 : 9$); (e) Sample 5 ($V_M : V_I = 1 : 12$); (f) Sample 6 ($V_M : V_I = 1 : 13$); (g) Sample 7 ($V_M : V_I = 1 : 15$); (h) Sample 8 ($V_M : V_I = 1 : 19$).

In summary, PS particles with diverse morphologies could be easily prepared by altering the ratio of V_M to V_I. As the ratio of V_M to V_I decreased, the surface roughness of PS particles increased, and size of PS particles decreased. In St/H_2O/EtOH ternary system, for $V_M : V_I \geq 1 : 2$, the spherical PS particles were obtained for $1 : 12 \leq V_M : V_I \leq 1 : 3$, the raspberry-like PS particles were prepared; for $1 : 19 \leq V_M : V_I \leq 1 : 13$, the hollow flower-like PS particles were synthesized.

3.2 Discussion on the mechanism of formation

Both experimental and theoretical studies evidenced that, ternary systems containing one hydrotrope (such as EtOH) and two immiscible fluids, both being soluble in the hydrotrope at any proportion, showed unexpected solubilization power and the presence of 'detergentless' microemulsions in such mixtures.[31–33,46] On the basis of these results, we proposed a plausible mechanism as shown in Scheme 2.

Generally, when the St/H_2O/EtOH ternary system reaches equilibrium, St monomers mainly exist in two phases. One is the EtOH–H_2O phase, in which St monomers exist mainly in a dissolved state.[31] The other is the oil phase, where St monomers are present in the form of long-lived small oil droplets.[24,28] The size of oil droplets is determined by the mass fraction of monomers in ternary systems.[25,27] The DLS was employed to characterize the size of oil droplets in ternary systems.[47] The oil droplets formed in the MM were 172 nm in diameter and had good monodispersity (Fig. 5a).

Based on thermodynamic theory, when the pressure, temperature and composition are constant, the final state of the system is completely determined. In order to observe the size evolution process of oil droplets in ternary systems, we developed two methods to obtain the ternary system with the same R. One is a direct mixing method, in which the EtOH was added to the styrene–water mixture. The other is an indirect mixing method, in which mixing MM with EtOH–H_2O mixture (wherein the volume of EtOH–H_2O mixture was represented as V_E and $V_{EtOH} : V_{H_2O} = 3 : 2$ in this mixture). Fig. 5 shows the DLS results

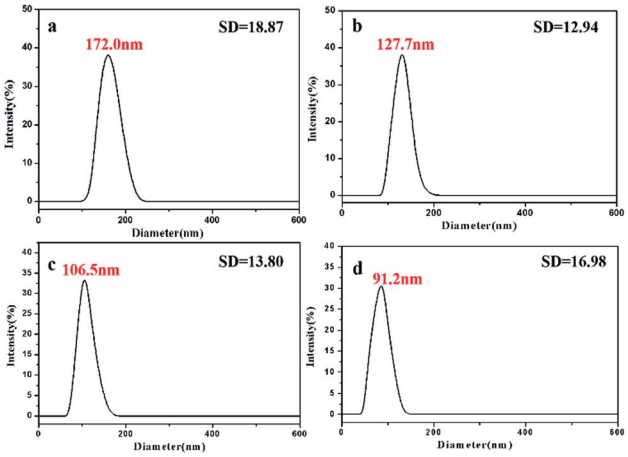

Fig. 5 DLS results of oil droplets in ternary systems with different R: (a) 2.95/44.34/52.71; (b) 0.34/45.58/54.08; (c) 0.24/45.63/54.13; (d) 0.21/45.64/54.15.

of oil droplets in ternary systems with different R obtained with the direct mixing method. For $R = 0.34/45.58/54.08$ (R is equal to that in the system of $V_M : V_E = 1 : 9$), the droplet size was 127.7 nm (Fig. 5b). For $R = 0.24/45.63/54.13$ (R is equal to that in the system of $V_M : V_E = 1 : 13$), the droplet size was 106.5 nm (Fig. 5c). For $R = 0.21/45.64/54.15$ (R is equal to that in the system of $V_M : V_E = 1 : 15$), the droplet size was 91.2 nm (Fig. 5d). Thus, as the concentration of St in ternary systems decreased, the size of oil droplets also decreased.[47]

Fig. 6 shows the evolution of size and distribution of oil droplets in the ternary system obtained by the indirect mixing method during the aging process. Mixing 10 mL MM ($R = 2.95/44.34/52.71$) with 90 mL EtOH–H_2O mixture ($V_M : V_E = 1 : 9$) at 25 °C, we obtained a new ternary system ($R = 0.34/45.58/54.08$). After aging for 20 min, the DLS curves of oil droplets became broader with standard deviation (SD) of 35.78 (Fig. 6a), and the size of oil droplets became larger (211.9 nm) compared to that of the MM (172.0 nm, Fig. 5a). This result indicated that the

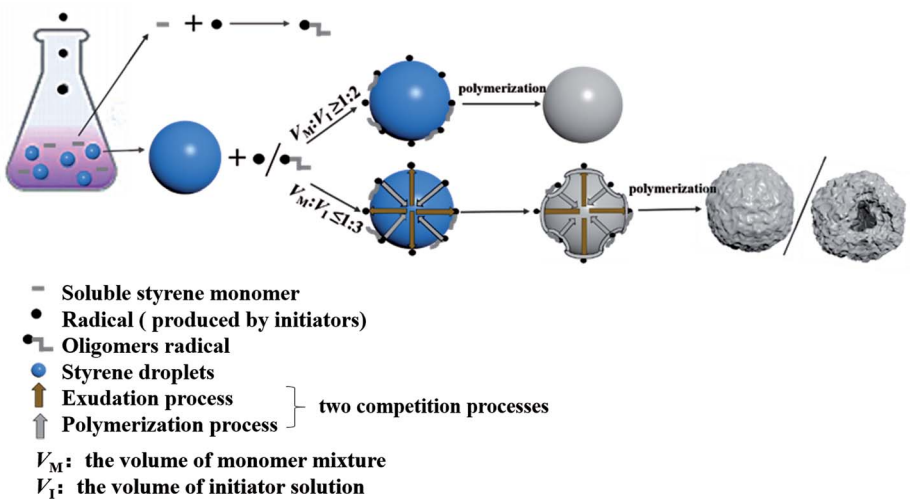

Scheme 2 Schematic diagram of the synthesis mechanism of PS particles with different morphologies.

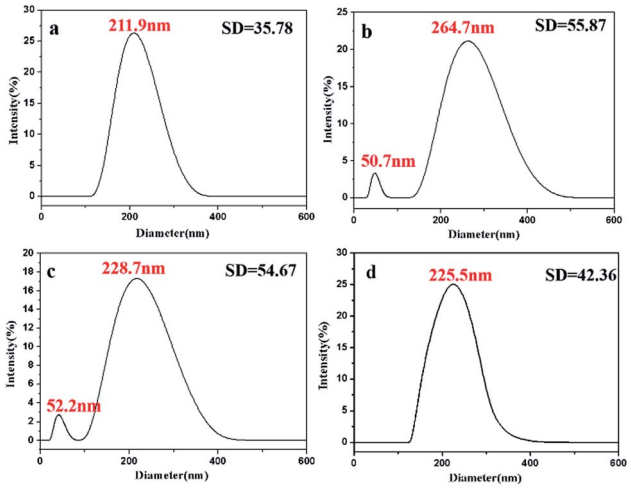

Fig. 6 DLS results of oil droplets in the ternary system prepared with $V_M : V_E = 1 : 9$ at different aging times: (a) 20 min; (b) 200 min; (c) 3600 min; (d) 5040 min.

change of oil droplets was happening. After aging for 200 min, a small peak appeared at 50.7 nm and it remained that way for at least 2.5 d (Fig. 6b). This phenomenon might be attributed to the exudate agglomeration.[26] After aging for 3600 min, the size of mean peak of oil droplets decreased (228.7 nm, Fig. 6c) compared to that of oil droplets aging for 200 min (264.7 nm, Fig. 6b). After aging for 5040 min (Fig. 6d), the small peak of oil droplets disappeared, and the size of mean peak decreased continuously (225.5 nm, Fig. 6d). Finally, when the new ternary system reached equilibrium, the size of oil droplets would be reduced to 127.7 nm ($R = 0.34/45.58/54.08$, Fig. 5b).

Similar results were observed for Sample 6 ($V_M : V_E = 1 : 13$, Fig. S5†) and Sample 7 ($V_M : V_E = 1 : 15$, Fig. S6†). Based on the results, we found that the exudation process was slow, and the exudation rate of substance in oil droplets were different. Taking the time corresponding to the appearance of the small peak in the curve as a reference (Fig. S7†), for $V_M : V_E = 1 : 9$, the small peak appeared at 200 min, whereas for $V_M : V_E = 1 : 13$, the peak appeared at 100 min. Finally, for $V_M : V_E = 1 : 15$, the peak appeared at 30 min. Therefore, it can be considered that the ratio of V_M to V_E affected the rate of material exudation from oil droplets, and the rate of exudation increased as the ratio decreased. This might be the important factors for the formation of diverse morphologies and even hollow structures of PS particles.

According to the principle of phase equilibrium in physical chemistry,[48] the chemical potential of St monomer in two phases is equal. When the EtOH–H_2O mixture is added to St/H_2O/EtOH ternary system which has already in equilibrium, the chemical potential of St in the oil phase do not change, but the chemical potential of St in the EtOH–H_2O phase decreased as the concentration decreased. As the addition of EtOH–H_2O mixture increases, the chemical potential of St decreases more significantly in the EtOH–H_2O phase. St monomer in the oil phase will seep out from oil phase into the EtOH–H_2O phase, bringing the ternary system to a new equilibrium (namely oil droplets can reach a new size).[38,39,42–45] The function of interfacial layer of oil droplets was similar to a permeable membrane, which can support the exchange of internal materials.[20] When the initiator solution was added to the MM instead of the EtOH–H_2O mixture, both exudation and polymerization processes would take place simultaneously. KPS initiated St monomers dissolved in the mixture to form the short oligomers. The short oligomers could be captured by the surface oil droplets to stabilize oil droplets.[34–37,40] The free radicals in the mixture could also be adsorbed onto the oil droplet surfaces. Therefore, the polymerization reaction could occur easily on the surface of oil droplets (Fig. 7).[44] At this point, there was a competition between the exudation process and polymerization process, resulting in the as-prepared PS particles with diverse morphologies. The addition of different volumes of initiator solution to MM would alter the competitive behaviors of these two processes, which leading to the production of PS particles with diverse morphologies.

3.3 Wettability of coatings assembled from PS particles with diverse morphologies

Based on the as-prepared PS particles with diverse morphologies, coatings assembled with the as-prepared particles were fabricated by vertical deposition method at 25 °C. Coatings with different thicknesses could be prepared by controlling the parameters of vertical deposition method.[29,30] However, investigations into the effect of thickness on the wettability of the coatings was not in the scope of this paper. Water contact angles of the coatings assembled with the as-prepared particles are presented in Fig. 8. For Sample 1 ($V_M : V_I = 1 : 0.15$, Fig. 8a), the water contact angle was around 62.5°. For Sample 4 ($V_M : V_I = 1 : 9$, Fig. 8b), the contact angle was increased to about 89.5°. For Sample 6 ($V_M : V_I = 1 : 13$, Fig. 8c), the contact angle was about 123.0°and it would be increased to 134.5° for Sample 7 ($V_M : V_I = 1 : 15$, Fig. 8d). Therefore, the water contact angles of the fabricated coatings increased as the ratio of V_M to V_I

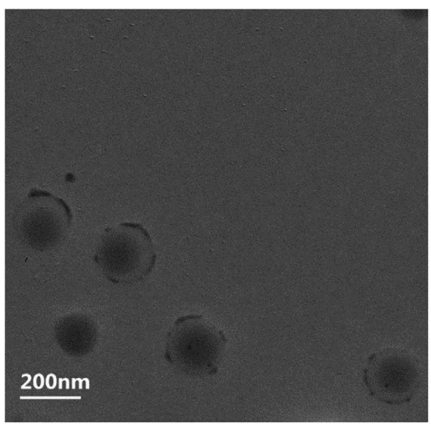

Fig. 7 TEM image of the polymerization process occured on the surface of oil droplets. The latex sample obtained after 10 min of polymerization, without any post-processing, was dropped onto a Formvar/carbon film coated grids and stored at 25 °C for electron microscopic analysis.

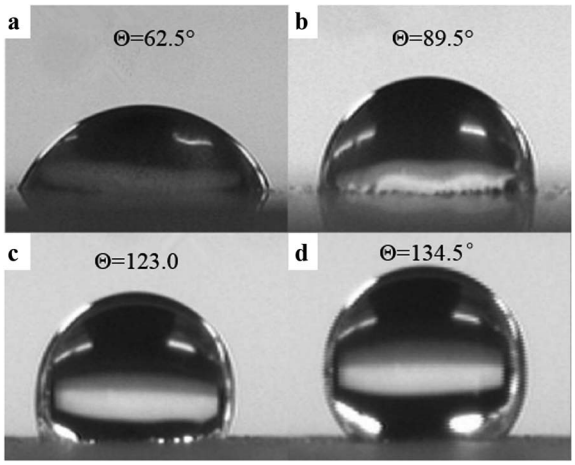

Fig. 8 The difference of water contact angle of the coatings assembled with the as-prepared particles: (a) Sample 1 ($V_M : V_I = 1 : 0.15$); (b) Sample 4 ($V_M : V_I = 1 : 9$); (c) Sample 6 ($V_M : V_I = 1 : 13$); (d) Sample 7 ($V_M : V_I = 1 : 15$).

decreased. The wettability of the coatings could be successfully tuned from hydrophilicity (Sample 1, 62.5°) to hydrophobicity (Sample 7, 134.5°) by varying the particles with different roughnesses.

4 Conclusions

In conclusion, PS particles with diverse morphologies were successfully synthesized by a simple, one-step, non-surfactant self-templating polymerization of St monomers in EtOH–H_2O mixture. The premixing of three components and altering the addition of initiator solution (namely altering the ratio of V_M to V_I) played key roles in controlling the morphologies. The as-prepared particles could be categorized as follows: for $V_M : V_I \geq 1 : 2$, the particles were spherical in shape; for $1 : 12 \leq V_M : V_I \leq 1 : 3$, the particles had raspberry-like structures; for $1 : 19 \leq V_M : V_I \leq 1 : 13$, the particles had hollow flower-like structures and controllable diameter (100–250 nm). The roughness of particles increased as the ratio of V_M to V_I decreased, whereas the size of the particles reduced correspondingly. The formation of as-prepared particles is determined by a competitive process of exudation and polymerization in oil droplets. Different volumes of initiator solution added to the monomer mixture would alter the competitive behaviors of these two processes, which leading to the as-prepared PS particles with diverse morphologies. The wettability of the coatings could be tuned from hydrophilicity to hydrophobicity by varying the particles with different roughnesses.

Conflicts of interest

There are no conflicts to declare.

Acknowledgements

This work was supported by Prof. Banglin Chen, Jianping Ge and Kun Zhang.

Notes and references

1 C. H. Chen, X. F. Li, D. Jiang, Z. Wang and Y. Wang, *ChemSusChem*, 2018, **11**, 2540–2546.
2 F. P. Dong, H. B. Xie and Q. Zheng, *RSC Adv.*, 2017, **7**, 6685–6690.
3 J.-W. Kim, R. J. Larse and D. A. Weitz, *Adv. Mater.*, 2007, **19**, 2005–2009.
4 J. B. Fan, Y. Song and H. Liu, *Sci. Adv.*, 2017, **3**, e1603203.
5 X. L. Fan and X. K. Jia, *Polym. Chem.*, 2015, **6**, 703–713.
6 S. Shi, T. Wang and Y. T. Tang, *Chin. Chem. Lett.*, 2011, **22**, 1127–1129.
7 J.-W. Kim, R. J. Larsen and D. A. Weitz, *Adv. Mater.*, 2007, **19**, 2005–2009.
8 X. M. Yang, T. Y. Dai and Y. Lu, *Polymer*, 2006, **47**(1), 441–447.
9 M. Chen, S. Zhou and B. You, *Macromolecules*, 2005, **38**, 6411–6417.
10 C. S. Wagner, S. Shehata and K. Henzler, *J. Colloid Interface Sci.*, 2011, **355**, 115–123.
11 Y. Zhang, H. Chen and X. Shu, *Colloids Surf., A*, 2009, **350**, 26–32.
12 D. Nagao, T. Ueno and D. Oda, *Colloid Polym. Sci.*, 2009, **287**, 1051–1056.
13 A. Perro, S. Reculusa and E.-L. Bourgeat, *Colloids Surf., A*, 2006, **284–285**, 78–83.
14 S. Reculusa, P.-L. Céline and S. Ravaine, *Chem. Mater.*, 2002, **14**, 2354–2359.
15 J. Huang, Q. Li and Y. Bao, *Colloid Polym. Sci.*, 2009, **287**, 37–43.
16 H. J. Tsai and Y. L. Lee, *Langmuir*, 2007, **23**, 12687–12692.
17 F. Dong, H. Xie, Q. Zheng and C. S. Ha, *RSC Adv.*, 2017, **7**, 6685–6690.
18 A. R. Goodall, M. C. Wilkinson and J. Hearn, *J. Polym. Sci., Part A: Polym. Chem.*, 2010, **15**, 2193–2218.
19 R. A. Cox, M. C. Wilkinson and J. M. Creasey, *J. Polym. Sci., Part A: Polym. Chem.*, 1977, **15**, 2311–2319.
20 A. R. Goodall, M. C. Wilkinson and J. Hearn, *J. Colloid Interface Sci.*, 1975, **53**, 327–331.
21 H. Lockie, R. Manica and R. F. Tabor, *Langmuir*, 2012, **28**, 4259–4266.
22 T. Yamamoto and S. C. Kim, *J. Polym. Res.*, 2017, **24**, 149.
23 Y. J. Wong, L. Zhu and W. S. Teo, *J. Am. Chem. Soc.*, 2011, **133**, 11422–11425.
24 G. François and J. L. Katz, *Chemphyschem*, 2010, **6**, 209–216.
25 L. M. Prince, *J. Colloid Interface Sci.*, 1967, **23**, 165–173.
26 L. M. Prince, *J. Colloid Interface Sci.*, 1969, **29**, 216–221.
27 G. D. Smith, C. E. Donelan and R. E. Barden, *J. Colloid Interface Sci.*, 1977, **60**, 488–496.
28 N. L. Sitnikova, R. Sprik and G. Wegdam, *Langmuir*, 2005, **21**, 7083–7089.
29 Y. G. Ko and D. H. Shin, *J. Phys. Chem. B*, 2007, **111**, 1545–1551.
30 A. S. Dimitrov and K. Nagayama, *Langmuir*, 1996, **12**, 1303–1311.
31 Z. Y. Li, H. Cheng and C. C. Han, *Macromolecules*, 2012, **45**, 3231–3239.

32 G. J. Kim, S. Lim, B. H. Lee and S. E. Shim, *Polymer*, 2010, **51**, 1197–1205.
33 C. T. Kresge, M. E. Leonowicz, W. J. Roth, J. C. Vartuli and J. S. Beck, *Nature*, 1992, **359**, 710.
34 X. L. Fan, X. K. Jia, H. P. Zhang and Q. Y. Zhang, *Langmuir*, 2013, **29**, 11730–11741.
35 X. P. Pei, K. K. Zhai, X. C. Liang and Y. K. Deng, *J. Colloid Interface Sci.*, 2018, **512**, 600–800.
36 W. C. Yan, M. W. Pan, J. F. Yuan and G. Liu, *Polymer*, 2017, **122**, 139–147.
37 M. Chen, L. M. Wu, S. X. Zhou and B. You, *Macromolecules*, 2004, **37**, 9613–9619.
38 R. Yan, Y. Y. Zhang, X. H. Wang and W. Q. Zhang, *J. Colloid Interface Sci.*, 2012, **368**, 220–225.
39 X. L. Fan, J. Liu, X. K. Jia and Q. Y. Zhang, *Nano Res.*, 2017, **10**, 2905–2922.
40 M. Chen, L. M. Wu, S. X. Zhou and B. You, *Macromolecules*, 2004, **37**, 9613–9619.
41 G. L. Li, X. L. Yang, F. Bai and W. Q. Huang, *J. Colloid Interface Sci.*, 2006, **297**, 705–710.
42 G. L. Li, X. L. Yang and J. Wang, *Colloids Surf., A*, 2008, **322**, 192–198.
43 Z. H. Nie, J. I. Park, W. Li and S. A. F. Bon, *J. Am. Chem. Soc.*, 2008, **130**, 16508–16509.
44 D. Z. Yin, X. Du, H. Liu, Q. Y. Zhang and L. Ma, *Colloids Surf., A*, 2012, **414**, 289–295.
45 D. Z. Yin, Q. Y. Zhang, C. J. Yin and X. B. Zhao, *Polym. Adv. Technol.*, 2012, **23**, 273–277.
46 W. Hou and J. Xu, *Curr. Opin. Colloid Interface Sci.*, 2016, **25**, 67–74.
47 X. Yan, P. Alcouffe, G. Sudre, L. David, J. Bernard and F. Ganachaud, *Chem. Commun.*, 2017, **53**, 1401.
48 P. W. Atkins and J. D. Paula, *Physical Chemistry*, Oxford University Press, 7th edn, 2002, ch. 6.